

An Agent-based Travel and Charging Behavior Model for Forecasting High-resolution Spatio-temporal Battery Electric Vehicle Charging Demand

Center for Transportation, Environment, and Community Health
Final Report



by

Yuechen Sophia Liu, Mohammad Tayarani, H. Oliver Gao

August 20, 2021

DISCLAIMER

The contents of this report reflect the views of the authors, who are responsible for the facts and the accuracy of the information presented herein. This document is disseminated in the interest of information exchange. The report is funded, partially or entirely, by a grant from the U.S. Department of Transportation's University Transportation Centers Program. However, the U.S. Government assumes no liability for the contents or use thereof.

1. Report No.	2. Government Accession No.	3. Recipient's Catalog No.	
4. Title and Subtitle An Agent-based Travel and Charging Behavior Model for Forecasting High-resolution Spatio-temporal Battery Electric Vehicle Charging Demand		5. Report Date August 20, 2021	
		6. Performing Organization Code	
7. Author(s) Yuechen Sophia Liu, Mohammad Tayarani, H. Oliver Gao		8. Performing Organization Report No.	
9. Performing Organization Name and Address School of Civil and Environmental Engineering Cornell University Ithaca, NY 14853		10. Work Unit No.	
		11. Contract or Grant No. 69A3551747119	
12. Sponsoring Agency Name and Address U.S. Department of Transportation 1200 New Jersey Avenue, SE Washington, DC 20590		13. Type of Report and Period Covered Final Report 5/21/2021-08/20/2021	
		14. Sponsoring Agency Code US-DOT	
15. Supplementary Notes			
16. Abstract <p>The expansion of the battery electric vehicle (BEV) market requires considerable changes in the supply of electricity to fulfill the charging demand. To this end, understanding the spatio-temporal distribution of BEV charging demand at a micro-level is crucial for optimal electric vehicle supply equipment (EVSE) planning and electricity load management. This research proposes an integrated activity-based BEV charging demand simulation model, which considers both realistic travel and charging behaviors and provides high-resolution spatio-temporal demand in real-world applications. Moreover, a novel charging choice model is proposed which provides more realistic demand modeling by allowing critical non-linearities in random utility to better describe observed charging behaviors. The results of a case study for the Atlanta metropolitan area imply that work/public charging has a substantial potential market, which can serve up to 64.5% of the total demand. Out of multiple charging modes, demand for direct-current fast charging (DCFC) is prominent at work/public, and it takes the largest portion of the non-residential demand in all simulation scenarios. Moreover, charging behaviors have significant impacts on the demand distribution. Comparing to risk-neutral users, high-risk sensitive users require 49% to 91% higher peak power demand of level 2 chargers at work/public. Users' preferences for fast charging rates can change DCFC demand from 36.4% to 53.7% of the total demand. This study helps to qualitatively analyze the factors of charging demand and their impacts on the demand distribution. The results can be directly used in EVSE planning and electricity load prediction.</p>			
17. Key Words Battery electric vehicle, Charging demand, Spatial-temporal distribution, Trip chain simulation, Charging behavior model		18. Distribution Statement Public Access TRB 2021 Annual Meeting	
19. Security Classif (of this report) Unclassified	20. Security Classif. (of this page) Unclassified	21. No of Pages	22. Price

Abstract

The expansion of the battery electric vehicle (BEV) market requires considerable changes in the supply of electricity to fulfill the charging demand. To this end, understanding the spatio-temporal distribution of BEV charging demand at a micro-level is crucial for optimal electric vehicle supply equipment (EVSE) planning and electricity load management. This research proposes an integrated activity-based BEV charging demand simulation model, which considers both realistic travel and charging behaviors and provides high-resolution spatio-temporal demand in real-world applications. Moreover, a novel charging choice model is proposed which provides more realistic demand modeling by allowing critical non-linearities in random utility to better describe observed charging behaviors. The results of a case study for the Atlanta metropolitan area imply that work/public charging has a substantial potential market, which can serve up to 64.5% of the total demand. Out of multiple charging modes, demand for direct-current fast charging (DCFC) is prominent at work/public, and it takes the largest portion of the non-residential demand in all simulation scenarios. Moreover, charging behaviors have significant impacts on the demand distribution. Comparing to risk-neutral users, high-risk sensitive users require 49% to 91% higher peak power demand of level 2 chargers at work/public. Users' preferences for fast charging rates can change DCFC demand from 36.4% to 53.7% of the total demand. This study helps to qualitatively analyze the factors of charging demand and their impacts on the demand distribution. The results can be directly used in EVSE planning and electricity load prediction.

Keywords

Battery electric vehicle, Charging demand, Spatial-temporal distribution, Trip chain simulation, Charging behavior model

1 Introduction

Greenhouse gas (GHG) emissions from the transportation sector are a major contributor to climate change [1, 2]. Among the major sources of GHG emissions, the use of fossil fuel in transportation has produced the largest portion (28%) of emissions in the U.S. since 2016, which accounts for more than 1,830 million metric tons of GHG each year [2]. Replacing fossil fuel used in transportation with climate-friendly energy sources is therefore one of the pressing imperatives for reducing long-term emissions [3, 4]. Among the alternatives to fossil fuel vehicles, battery electric vehicles (BEVs), vehicles that are powered purely by electricity and produce zero emissions when in use, have emerged as a potential reliable solution to a future zero-emission transportation system [5, 6, 7, 8].

The BEV market has been expanding rapidly in the past ten years. The BEV market share in the U.S. has experienced considerable expansion since 2011, by an average annual growth rate of 48.8% [9]. Until 2019, the U.S. BEV annual sales have increased up to 242,000, and counted for 1.5% of the annual light-duty vehicle sales [9]. Although the overall BEV market penetration rate is still moderate, it is expected that the market to continue booming [10]. Nationwide financial incentive policies, such as tax credit, are effectively increasing the growth of the BEV market [11]. Furthermore, more aggressive policies to phase-out of fossil fuel vehicles, such as the New York State's legislation which requires the sales of all new passenger vehicles and light trucks to be zero-emission by 2035, would largely increase the market share of BEVs. Under these circumstances, the number of nationwide registered BEVs is predicted to be 7.5 million in 2030 [12], which counts for 10% of the light-duty vehicle market share. When fossil fuel vehicles gradually phase out, it is anticipated that BEV would become prominent among passenger vehicles in the near future.

The expansion of the BEV market, however, calls for a more rapid increase in electricity charging demand [13], thereby bringing new challenges for both electric vehicle supply equipment (EVSE, also known as electric vehicle charging infrastructure) planning and electricity load management [14]. The BEV charging demand is expected to rise to 153 *TWh* in the U.S. in 2030, counting up to 4% of the nation's yearly electricity consumption [15]. This presents both economic benefits and challenges in infrastructure planning and electricity load management. For infrastructure planning, misplacement of EVSEs at low-demand locations could lead to low utilization rates and investment failure. For electricity load management, additional demands for electricity, especially during peak hours, could exceed the maximum supply capacity and cause regional power outages. Thus, accurately estimating the spatio-temporal distribution of the BEV's charging demand is crucial to achieving optimal EVSE planning and electricity load management.

In the existing literature, analyzing historical charging event data is the most common method to study BEV's charging demand; even though it may not be an accurate measure of the future demand. For instance, Ref. [16] forecasts the charging load by consumers' charging records and stations' records. The key characteristics of charging events and demands are analyzed by machine learning methods, such as Gaussian mixture models, clustering, and fuzzy logic models [17, 18]. However, because the current BEV adoption rate is still moderate and low EVSE coverage is limiting charging in public areas, the historical charging event data at this stage may not be a true indicator of future charging demand.

In previous studies, travel demand modeling is widely adopted to estimate charging demand. In the literature, trip chain (a series of linked trips) simulation is regarded as a key method for studying charging demand [19, 20, 21, 22, 23, 24, 25, 26]. Travel characteristics, such as daily driving patterns and distances, are taken as the main attributes to estimate charging demand [27, 28, 29, 30, 31, 32]. Although these methods have been shown to reasonably describe the mobility behavior of BEVs [33], travel demand cannot fully represent charging demand. Because users may not charge equally at every destination, and the charging demand would only appear at the destinations where users choose to charge. Thus, users' charging behavior plays a critical role when estimation charging demand.

Although users' charging behavior is another main factor affecting charging demand [34, 35], most previous charging demand research makes simplified behavioral assumptions. Some research assumes charging behavior is deterministic considering fixed charging strategies [28, 23]. Other research addresses random charging behavior by applying fuzzy logit models for charging probability [18, 22, 36, 37]. Fuzzy logit models can represent the relative change of charging probability, but they cannot precisely evaluate the effect of charging mode attributes on charging behavior. Several studies describe charging behavior using discrete choice models with linear utility [38, 39], which can capture the weighted effect of each parameter. This approach, however, may not be accurate since some attributes, such as state of charge

(SOC), are non-linearly related to charging decisions. If non-linearity is uncaptured, the charging demand could be overestimated at places where it provides more charging options.

Despite the importance of understanding the high-resolution spatial distribution of charging demand in the real-world for EVSE planning, there is relatively little evidence about it in the literature. Some studies estimate spatial charging demand by travel purpose categories [24, 25]. Other research provides spatial demand on a toy model with fictitious areas representing activity types [21, 22]. Extending these methods to a more realistic set of locations, however, is impractical as areas typically are associated with a range of activities, making it difficult to tag an area by a single purpose. Ref. [28] and Ref. [40] estimate spatial distribution by dwell time at destinations and travel behavior by regions, without addressing individuals' travel activities and charging behaviors.

This research attempts to fill the aforementioned gaps through building a BEV charging demand simulation model and analyzes the demand distribution through considering scenarios with various charging behaviors in a future mature market. Our study contributes to the existing literature in several ways. First, this study proposes a modeling framework for integrated activity-based BEV charging demand simulation, which considers both realistic travel and charging behaviors and can be generally adopted with broad real-world applications. Second, the research constructs a novel charging behavior model for charging mode choice, which gives a more realistic estimation by capturing non-linear changes in random utility and charging behavior observations from the state of the art. Third, various charging choice factors, namely risk sensitivity, preference to charging rate and charging availability rate are scrutinized, which are shown to have various impacts on charging demand distribution. Lastly, this study also provides the high-resolution spatio-temporal distribution of charging demand in a real-world case, which can be directly useful for EVSE planning and electricity load management.

The rest of the paper is organized as follows. Section 2 provides details of the charging demand simulation model. Section 3 describes the case study settings. Section 4 presents the results of the case study and the implication of the research. Finally, Section 5 summarizes the study and discusses future research directions.

2 Methodology

The modeling framework is depicted in Fig. 1. The inputs include the household travel surveys (HTS) data, regional shapefiles, BEV and EVSE market settings, and charging behavior scenarios. Each user's trip chain, charging choice at each destination, and charging demand are simulated sequentially. Then regional charging demand is computed by accumulating users' demand. Details of each module are presented in this section.

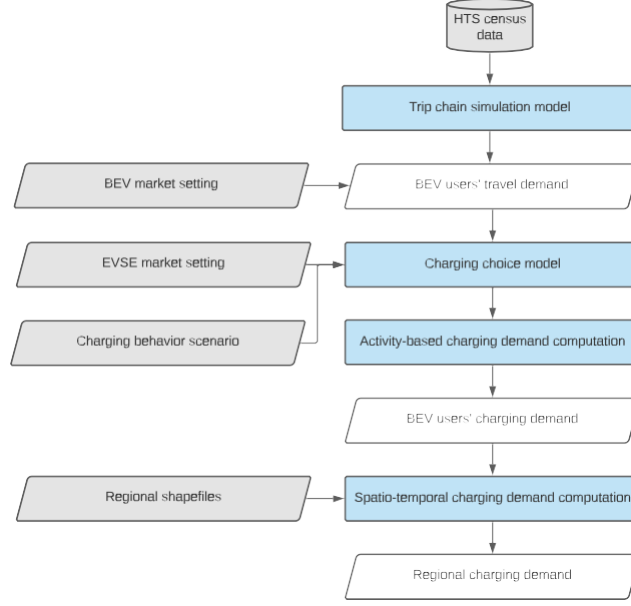


Figure 1: Flowchart of the simulating process. Input data are in grey. Blue boxes depict modeling processes. Output data are in white.

2.1 Trip chain simulation model

Trip chains are used to describe the travel patterns of BEVs. We assume there are N agents, each one representing a BEV. A trip chain (TC_n) for the n^{th} BEV is defined as

$$TC_n = [T_{n1}, T_{n2}, \dots, T_{nl}, \dots, T_{nm(n)}], \quad (1)$$

where $m(n)$ represents the total number of trips of the n^{th} BEV. T_{nl} is the l^{th} trip of the n^{th} BEV, which is defined by a list of attributes:

$$T_{nl} = [TAZ_{nl}, Pu_{nl}, Ts_{nl}, Tt_{nl}, Tl_{nl}, Te_{nl}, Td_{nl}, D_{nl}]. \quad (2)$$

These attributes are explained in details below. In general, they can be extracted via an agent-based travel demand model. For example, this research adopts the travel demand model by the Atlanta Regional Commission (ARC ABM).

The ARC ABM is composed of a Coordinated Travel-Regional Activity Modeling Platform (CT-RAMP) and a user equilibrium traffic assignment model and details of the ARC ABM are explained in Ref. [41], and here we summarize what the attributes are in Equation 2, and how they are computed in the ARC ABM model. CT-RAMP uses HTS as input data and contains a series of multinomial logit models. In the first step of the CT-RAMP model, synthetic household and population distribution for the modeling year are created for each traffic analytic zone (TAZ), which is a geographic unit built from census blocks. At an individual level, the origin of the trip chain is set to be at the home location. Then, three types of activities (mandatory, maintenance, and discretionary) are considered sequentially. The travel frequency, travel purpose (Pu_{nl}), and start time (Ts_{nl} in every 30-minute interval) of mandatory trips, such as work and school, are modeled first based on the individual's employment status. Travel purpose and start time of maintenance and discretionary trips are scheduled in the residual time window after scheduling the mandatory trips. The destination zone (TAZ_{nl}) of each trip is further modeled by the household's and individual's characteristics, type of the activity, trip start time, etc. Then, a user equilibrium traffic assignment modeled by Citilabs' Cube Voyager software is used to assign these trips to the transportation network and obtain the travel time (Tt_{nl}) and distance (Tl_{nl}).

Then, trip end time (Te_{nl}) is derived by adding the travel time to trip start time:

$$Te_{nl} = Ts_{nl} + Tt_{nl}. \quad (3)$$

Dwelling time (Td_{nl}) is computed by the duration from trip end time until the next trip's start time:

$$Td_{nl} = Ts_{n(l+1)} - Te_{nl}. \quad (4)$$

Destination type (D_{nl}) is classified into 3 categories (home, work, and public) and decided by the trip purpose:

$$D_{nl} = \begin{cases} \text{home,} & \text{if } Pu_{nl} = \text{home,} \\ \text{work,} & \text{if } Pu_{nl} = \text{work,} \\ \text{public,} & \text{if else.} \end{cases} \quad (5)$$

2.2 Charging choice model

We assume charging can happen at the end of each trip. The charging decision is made based on the availability of EVSEs, SOC of the BEV, and characteristics of charging modes (types of EVSE). If a charging mode is chosen, the BEV begins charging after arrival and stops charging when the next trip starts or the BEV is fully charged [33, 42]. For the n^{th} BEV, at the end of each trip T_{nl} , a charging mode L_{nl} is sampled according to the choice probability of each charging mode ($P_{\text{choice}_{nl}}$):

$$L_{nl} \sim P_{\text{choice}_{nl}}. \quad (6)$$

2.2.1 EVSE availability

We assume the available charging modes depend on the type of location. At home, level 2 home charging is available; meanwhile, at work/public location, level 2 charging and direct-current fast charging (DCFC) may be available. An example setting of charging mode is shown in Section 3.2 Table 2. We define a Bernoulli distribution to describe the discrete probabilities of whether a charging mode is available. Here we assume $L_{i,nl} = 1$ means charging mode i at the end of trip T_{nl} is available, and $L_{i,nl} = 0$ represents it is not available. $L_{i,nl}$ is drawn from the Bernoulli distribution:

$$L_{i,nl} \sim \text{Bernoulli}(Pl_{i,nl}), \quad (7)$$

where $Pl_{i,nl}$ is the availability rate of charging mode i after trip T_{nl} , which is determined by the type of destination. For the other charging mode $L_{i,nl}$, the availability depends on the destination type D_{nl} . We assume charging is always available at home location.

2.2.2 Charging mode choice model

The choice set C_{nl} after trip T_{nl} includes all available charging modes. The charging choice over available charging modes is modeled by a conditional logit model, which estimates the choice probabilities of discrete alternatives by comparing customers' preferences described by random utilities [43]. The random utility for each charging mode $L_{i,nl}$ is then defined as

$$U(L_{i,nl}) = V(L_{i,nl}) + \varepsilon(L_{i,nl}), \quad \forall i \in C_{nl}, \quad (8)$$

where $V(L_{i,nl})$ is indirect utility modeled by attributes of charging mode $L_{i,nl}$ and $\varepsilon(L_{i,nl})$ is an error term.

Following the principle of choosing the alternative with the maximum utility, the probability of choosing charging mode $L_{i,nl}$ is derived by comparing the utility of every alternative

$$\begin{aligned} P_{\text{choice}_{nl}}(L_{i,nl}) &= P(U(L_{i,nl}) \geq U(L_j^{nl}), \quad \forall j \in C_{nl}, \quad i \neq j) \\ &= P(\varepsilon(L_j^{nl}) - \varepsilon(L_{i,nl}) \leq V(L_{i,nl}) - V(L_j^{nl}), \quad \forall j \in C_{nl}, \quad i \neq j). \end{aligned} \quad (9)$$

Assuming each error term follows extreme value type 1 distribution $\varepsilon(L_{i,nl}) \sim EV1(0, 1)$, the choice probability of each charging mode is derived to a closed-form [43]:

$$P_{\text{choice}_{nl}}(L_{i,nl}) = \begin{cases} \frac{\exp(V(L_{i,nl}))}{\sum_{j \in C_{nl}} \exp(V(L_j^{nl}))}, & \text{if } i \in C_{nl}, \\ 0, & \text{if } i \notin C_{nl}. \end{cases} \quad (10)$$

For the not charging choice, the indirect utility is normalized to 0:

$$V_{L_0^{nl}} = 0. \quad (11)$$

The indirect utility for each charging mode depends on its attributes, which is further explained in the following section.

2.2.3 Decision attributes and indirect utility of charging mode

According to the existing literature, a user's choice of charging mode depends on the end of trip SOC (the percentage of electric capacity left in the BEV), preference over the charging rate (charging power, in kW/h), increase of SOC after charging, and cost (in \$). Table 1 summarizes the observed charging behaviors from previous studies.

Table 1: Observed charging behaviors from literature.

Attributes	Observed behaviors
End of trip SOC	Range buffer: the minimum SOC level users want to maintain [44, 45]. Risk sensitivity: the change of charging probability when SOC decreasing [42].
Charging rate	Positively affect charging choice, if willing to reduce charging duration [46]. Negatively affect charging choice, if concern about battery deterioration [47].
Increase of SOC	Positively affect users' charging choice [48].
Cost	Negatively affect charging choice [46, 49, 50]. If the cost is lower than charging at home, users prefer to charge [46].

To capture the observed behaviors, this research models the indirect utility of charging level $L_{i,nl}$ by the observed attributes listed above. The indirect utility of charging mode $L_{i,nl}$ is defined as

$$V(L_{i,nl}) = \beta_0 + V(\text{SOC}_{nl}^e) + V(R(L_{i,nl})) + V(\Delta\text{SOC}(L_{i,nl})) + V(\text{Cost}(L_{i,nl})), \quad i \in C_{nl} \setminus \{0\}, \quad (12)$$

where β_0 is the constant to represent the average effect of uncaptured attributes. Each component, V_X , represents the utility of the observed attribute X .

End of trip SOC (SOC_{nl}^e) is the main attribute determining whether or not to charge [21, 33]. An agent's charging decision depends on a range buffer, which is the minimum SOC level users want to maintain [44, 45]. If the end of trip SOC is lower than the range buffer, users tend to charge [51]; otherwise, users tend not to charge. On the other hand, risk sensitivity is defined as the changes in the user's charging preferences when SOC decreasing [42].

As SOC is the percentage of electric capacity within [0%, 100%], a set of realistic behaviors need to be considered: if the end of trip SOC is high and approximately 100% (the BEVs are almost fully charged), the user's charging probability is low and approximately 0; if the end of trip SOC is low and approximately 0% (i.e., users have a concern of not finishing the next trip), the user's charging probability is high and approximately 1.

To capture both the observed and boundary behaviors described previously, we propose the indirect utility for the end of trip SOC as

$$V(\text{SOC}_{nl}^e) = \begin{cases} +\infty, & \text{if } \text{SOC}_{nl}^e = 0, \\ \beta_{\text{SOC}} \cdot \ln\left(\frac{1 - \text{SOC}_{nl}^e}{(\frac{1}{\text{SOC}_B} - 1) \cdot \text{SOC}_{nl}^e}\right), & \text{if } \text{SOC}_{nl}^e \in (0, 1), \\ -\infty, & \text{if } \text{SOC}_{nl}^e = 1, \end{cases} \quad (13)$$

where SOC_B is the range buffer. When the end of trip SOC is larger than the range buffer, it negatively affects charging choice; otherwise, it positively affects charging choice. β_{SOC} represents the level of risk sensitivity.

Charging rate has a more nuanced impact on charging choice behavior [46]. Because high charging power may lead to battery deterioration [47], it is believed that users tend to avoid faster charging. However, some research finds users would prefer to reduce charging duration [46], thus preferring faster charging. This may be because the battery deterioration concern is not well-known among current BEV users, but users' preferences for charging rate are possible to shift when more BEVs are adopted. Thus, the effect of attitude change towards charging rate is scrutinized in the following sections. In this research, we assume the charging rate is linearly related to indirect utility of charging [42]. The form of utility is expressed as

$$V(R(L_{i,nl})) = \beta_R \cdot (R(L_{i,nl}) - R_{\text{home}}), \quad (14)$$

where $R(L_{i,nl})$ is the charging rate of charging mode $L_{i,nl}$, R_{home} is the charging rate at home. β_R represents the marginal utility of charging rate, which is also the willingness to pay/accept for charging rate as we model in the willingness to pay space. If users have a willingness to pay for charging rate ($\beta_R > 0$) and $R(L_{i,nl})$ is higher than home charging rate, users prefer to charge with the higher rate; otherwise, their preference is inverse.

Increase of SOC ($\Delta\text{SOC}(L_{i,nl})$) represents the increased percentage of electric capacity if charging with mode $L_{i,nl}$. It is calculated as

$$\Delta\text{SOC}(L_{i,nl}) = \min\left(\frac{Rl_i \cdot Td_{nl}}{E_n}, 1 - \text{SOC}_{nl}^e\right), \quad (15)$$

where Rl_i is charging rate of charging mode $L_{i,nl}$, E_n is the electric capacity of the n^{th} BEV, and SOC^e is the end of trip SOC.

The increase of SOC positively affects users' charging choice [48]. Meanwhile, when a small amount of energy is charged, the user would be eager to charge more. And when a large amount of energy has been charged, the user's satisfaction remains high but stable. these mean the marginal utility of $\Delta\text{SOC}(L_{i,nl})$ is positive and decreases when $\Delta\text{SOC}(L_{i,nl})$ is high. To capture the marginal utility change, we use a quadratic form to describe the indirect utility of $\Delta\text{SOC}(L_{i,nl})$:

$$V(\Delta\text{SOC}(L_{i,nl})) = \beta_{\Delta\text{SOC}} \cdot [1 - (\Delta\text{SOC}(L_{i,nl}) - 1)^2]. \quad (16)$$

$\text{Cost}(L_{i,nl})$ is the total charging cost of using charging mode $L_{i,nl}$, which is calculated by the charging energy and charging price rate P_{L_i} (in $\$/kWh$):

$$\text{Cost}(L_{i,nl}) = P_{L_i} \cdot \Delta\text{SOC}(L_{i,nl}) \cdot E_n. \quad (17)$$

Previous research concludes users prefer a charging mode if the cost is lower [49, 50], especially if the cost is lower than charging at home [46]. Thus, we model the indirect utility of cost as

$$V(\text{Cost}(L_{i,nl})) = -\beta_{\text{Cost}} \cdot (\text{Cost}(L_{i,nl}) - \text{Cost}_{\text{home}}), \quad (18)$$

where β_{Cost} is the marginal utility of cost. To model in the willingness to pay space, we assume $\beta_{\text{Cost}} = 1$ in the following sections. $\text{Cost}_{\text{home}}$ is the total charging cost when an equal amount of energy is charged at home:

$$\text{Cost}_{\text{home}} = P_{\text{home}} \cdot \Delta\text{SOC}(L_{i,nl}) \cdot E_n. \quad (19)$$

2.3 Activity-based charging demand

The charging demand of each agent is calculated after each charging decision. The n^{th} BEV travels follow the trip chain TC_n . After each trip T_{nl} , the end of trip SOC is computed by the trip's start SOC minus the SOC declination during the trip T_{nl} :

$$\text{SOC}_{nl}^e = \text{SOC}_{nl}^s - \frac{c_n \cdot Tl_{nl}}{E_n}, \quad (20)$$

where c_n is the energy consumption rate (in $kWh/mile$) of the n^{th} BEV, Tl_{nl} is the travel distance of trip T_{nl} , and E_n is the electric capacity of the n^{th} BEV.

Assuming the BEV is charged by constant charging rate r_{nl} of the chosen charging mode L_{nl} until the maximum dwelling time or fully charged, the charging time $T_{\text{charge}_{nl}}$ is computed by

$$T_{\text{charge}_{nl}} = \begin{cases} \min\left(\frac{E_n \cdot (1 - \text{SOC}_{nl}^e)}{r_{nl}}, Td_{nl}\right), & \text{if } r_{nl} \neq 0, \\ 0, & \text{if } r_{nl} = 0. \end{cases} \quad (21)$$

Power demand (in kW) at time t , $\text{power}_{nl}(t)$, is equal to the chosen charging rate r_{nl} during the charging time:

$$\text{power}_{nl}(t) = \begin{cases} r_{nl}, & \text{if } Te_{nl} \leq t \leq Te_{nl} + T_{\text{charge}_{nl}}, \\ 0, & \text{if else.} \end{cases} \quad (22)$$

Energy demand E_{nl} (in kWh), the accumulated electricity demand during the dwelling time, is the constant charging rate multiplied by the charging time:

$$E_{nl} = \int_{T_{e_{nl}}}^{T_{e_{nl}}+T_{d_{nl}}} \text{power}_{nl}(t) dt = r_{nl} \cdot T_{\text{charge}_{nl}}. \quad (23)$$

At the end of a dwelling time, the start SOC of the next trip ($\text{SOC}_{n(l+1)}^s$) is calculated by adding the end of trip SOC to the increase of SOC after charging:

$$\text{SOC}_{n(l+1)}^s = \text{SOC}_{nl}^e + \frac{E_{nl}}{E_n}. \quad (24)$$

2.4 Spatio-temporal charging demand

After simulating the charging demand of each BEV for the study period, the accumulated spatio-temporal distribution of charging demand is calculated. Given each sub-area TAZ_i , the regional power demand at time step t , $\text{power}_{\text{TAZ}_i}(t)$, is the accumulation of individual power demand at the same TAZ:

$$\text{power}_{\text{TAZ}_i}(t) = \sum_{T_{nl}, \forall \text{TAZ}_{nl}=\text{TAZ}_i} \text{power}_{nl}(t). \quad (25)$$

The regional energy demand at TAZ_i (E_{TAZ_i}) is the accumulation of individual energy demand at the same TAZ

$$E_{\text{TAZ}_i} = \sum_{T_{nl}, \forall \text{TAZ}_{nl}=\text{TAZ}_i} E_{nl}. \quad (26)$$

3 Case study

3.1 Study area and trip data

The Atlanta metropolitan area is used in the case study. It is the third-largest metropolitan region in the southeast of the U.S. and the fourth fastest growing metropolitan area in the U.S.

The HTS collected by the Georgia Department of Transportation (GDOT) in 2011 is used as the input data of ARC ABM. Then individual trip data for the year 2030 is simulated by the ARC ABM, which contains 4.9 million vehicles and 21.3 million typical commute trips [41]. We assume the BEV penetration rate is 10% in 2030 [12]. Thus, 10% of the vehicles are randomly chosen and their simulated trip-chain data are used in the case study, which includes 494,398 vehicles and 2,132,248 typical commute trips on a normal weekday.

Fig. 2 represents the 11 counties and 5966 TAZs of the Atlanta metropolitan area. The color shows the number of trips arrived at each TAZ, where darker blue corresponds to more trips ending in the TAZ. The TAZs with especially high travel demand tend to contain special points of interest. For example, the dark blue TAZ in the north-west of Clayton county contains the Atlanta international airport.

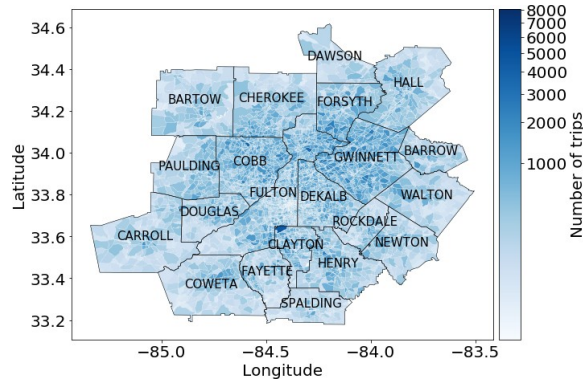


Figure 2: Counties and number of trips end at each TAZ of the Atlanta metropolitan area.

3.2 Market setting

In the case study, we assume the BEV market is composed of 3 groups of BEV with different market shares [12]. Table 2 lists the electric capacity and energy consumption rate of each group used in the simulation.

Table 2: Market share and parameters of BEV groups.

	BEV group 1	BEV group 2	BEV group 3
Model examples	Nissan Leaf, Fiat 500e	Tesla Model S, Chevrolet Bolt	Tesla Model X
Market share	30%	60%	10%
Electric capacity E_n (kWh)	40	100	100
Energy consumption rate C_n (kWh/mi)	0.3	0.3	0.35

We assume users have level 2 charging with 3.6 kW charging rate at home, and work/public places may offer 2 possible options: level 2 charging with 6.2 kW and DCFC with 150 kW [12]. The charging price is set to be 1.1 \$/kWh at home [52], and charging elsewhere is 20% more expensive than at home.

Table 3: Charging mode at different location types.

Location	Charging mode	Charging rate (kW)
Home	L2 home	3.6
Work/Public	L2	6.2
Work/Public	DCFC	150

3.3 Charging behavior scenarios

A number of simulation studies are conducted to examine the effect of varying preferences on charging choice. Five charging behavior scenarios are designed to compare the effect of risk sensitivity and preference to charging rate. A base case is designed to represent the medium risk sensitivity and no preference for fast charging. Two more risk sensitivity scenarios are designed. In a high-risk sensitivity scenario, users are very sensitive to SOC decreasing and their probability of charging quickly increases as long as the BEV is not fully charged. In a low-risk sensitivity scenario, users only start charging when the SOC approximates the range buffer. Two other scenarios are designed to analyze the distinct attitudes towards charging rate. A scenario of willingness to pay for charging rate covers the case when charging rate positively affects charging choice; a scenario of willingness to accept for charging rate represents the case when the effect of charging rate is negative. 5 provides the parameters in each scenario.

3.4 Simulation process

In the simulation process, every BEV's charging demand in a 24-hour period is simulated for each charging behavior scenario. At the beginning of the simulation, the initial SOC of each BEV in the first day is drawn from a truncated normal distribution ranged in [30%, 100%] with a mean of 65% and variance of 0.2. To eliminate the effect of this initial SOC setting, so-called burn-in periods are used; several consecutive days are simulated and the following day's initial SOC is obtained from the previous day's final SOC and overnight charging decision, until the distribution of each day's initial SOC remains stable [33]. All but the last period are discarded. The simulation results suggest the distribution of the initial SOC reaches stability after four or five days (depending on the charging behavior scenarios). Thus, we use the results of the sixth day for analysis.

4 Results & discussion

4.1 Spatio-temporal distribution of charging demand

The energy demand at home spreads relatively evenly in the study area, while the energy demand at work/public is more concentrated at specific TAZs in Fig. 3. Contrasting Fig. 3 with the trip destination frequency in Fig. 2, the spatial distribution of demand is highly related to the regional travel pattern. Especially the level 2 energy demand at work/public is highly concentrated in areas with high travel demand. This is expected as we assume charging happens at the trip destination in this research. However, the magnitude of demand at each TAZ is highly affected by charging choice, which is explored in the following section.

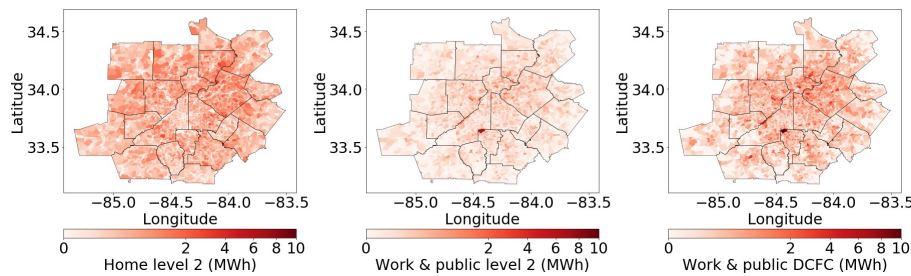


Figure 3: Spatial distribution of energy demand by charging mode (base case).

The peak power demand of each charging mode appears at different times. Fig. 4 tabulates the power demand by charging modes for times 9:00, 18:00, and 22:00, respectively. At 9:00 (row 1), low power demand appears at home, but work/public areas provide the highest power demand during the day. In particular, level 2 power demand at work/public spreads over morning destinations but DCFC power demand is highly concentrated at a limited number of TAZs. At 18:00 (row 2), the power demand at home increases and spreads over the residential areas. Meanwhile, level 2 power demand at work/public diminishes, and DCFC power demand remains high but shifts to another group of TAZs. At 22:00 (row 3), home power demand is dominant.

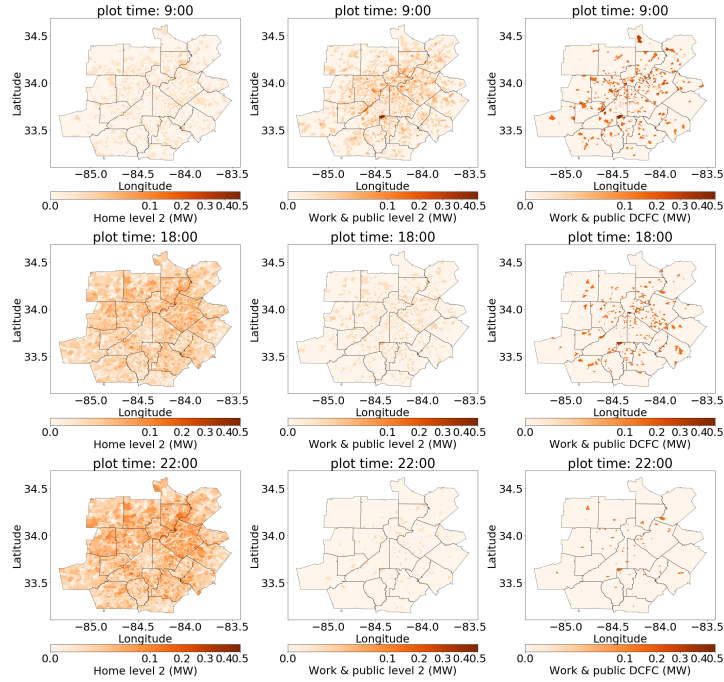


Figure 4: Power demand by charging mode at 9:00, 18:00, and 22:00 (base case).

4.1.1 Evaluation of the simulation results of charging behavior

The distribution of simulated initial charging SOC is presented in Fig. 5. Ref. [33] proves that the initial charging SOC is normally distributed with mean μ in $[0, 1]$ and variance σ in $[0, 0.5]$. The initial charging SOC in our simulation (base case for example) is normally distributed with mean $\mu = 0.6$ and $\sigma = 0.1$, which is consistent with the result by Ref. [33].

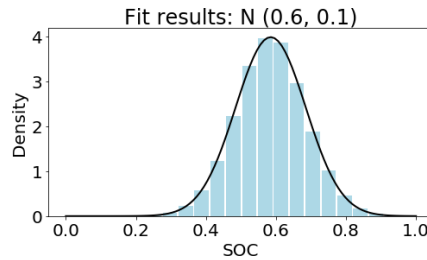


Figure 5: Initial charging SOC distribution (base case).

4.2 Sensitivity analysis

4.2.1 Effect of risk sensitivity

A high-risk sensitivity can shift 5.3% charging demand from home to work/public places and decrease the peak power demand at home from $110M W$ to $91.3M W$ in Fig. 6. This is because high-risk sensitive users tend to keep their SOC at a higher average level by charging their BEVs more frequently with an average of 0.6 times/day for each BEV. Whereas the average decreases to 0.3 and 0.2 times/day for medium and low-risk sensitivity scenarios, respectively. The more frequent charging leads to more use of work/public EVSEs and higher demand at work/public.

The DCFC demand at public is prominent (28.2%-28.7% of total demand) in all three scenarios, although a high-risk sensitivity increases the variation in power at DCFC in Fig. 6. This is also driven by high-risk sensitive users charging more frequently to maintain a high SOC. The results show that the average initial charging SOC is 90%, 60%, and 40% for the high, medium, low-risk sensitivity scenarios,

respectively. Moreover, high initial charging SOC makes the charging duration, especially at DCFC, much shorter in the high-risk sensitivity scenario compared to the low sensitivity one. These also introduce more variation in power demand since an increased number of BEVs plug in more frequently for shorter durations.

Fig. 6 also presents that a high-risk sensitivity increases the peak power demand of level 2 at both work and public, while it decreases the DCFC demand at work. The increase of level 2 demand is mainly because high-risk sensitive users charge more frequently in general. As their initial charging SOC is relatively high, much less energy would be needed once they start charging. This makes DCFC less attractive at work locations.

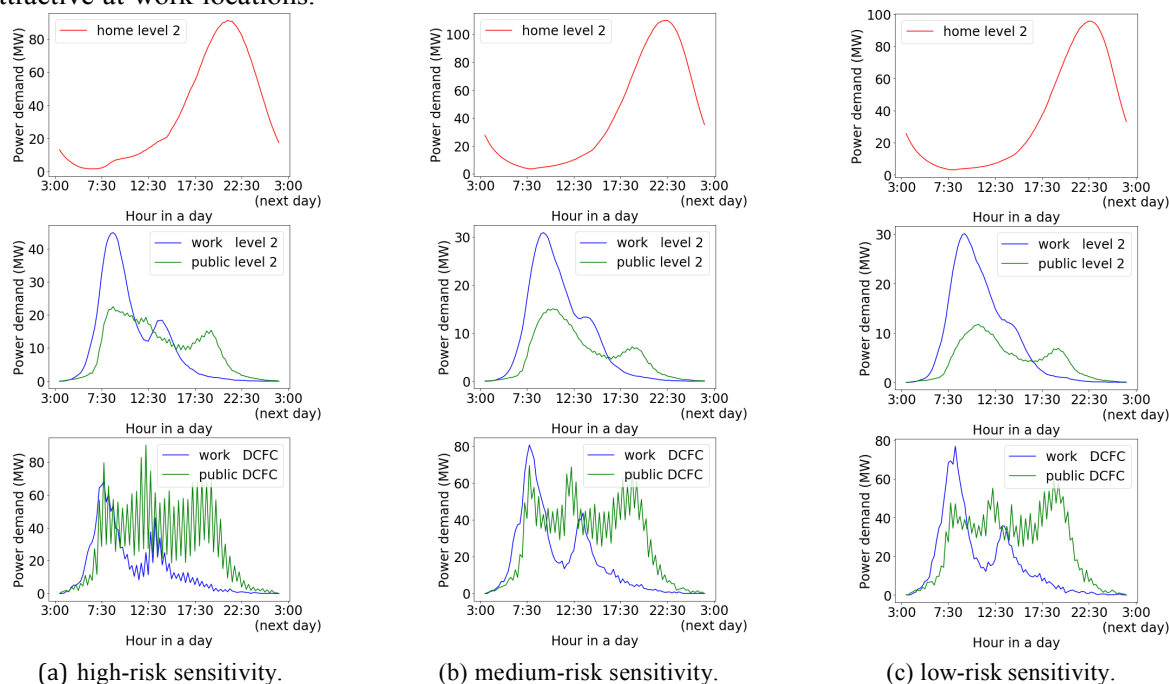
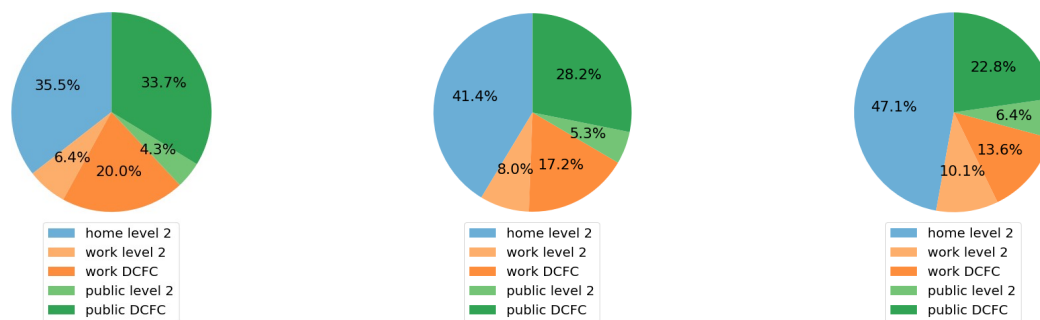


Figure 6: Power demand in 24 hours of three scenarios with different risk sensitivities.

4.2.2 Effect of preference to charging rate

The DCFC demand is dominant at work/public locations in all scenarios, even when users have a dislike for fast charging rates. As in Fig. 7, when users have a preference for fast charging rates, the demand share of DCFC is the highest, and takes more than half of the total demand (53.7%). Surprisingly, even when users have a dislike for fast charging rates, DCFC still takes up to 36.4% of the total demand, which is higher than the demand share of level 2 at work/public. This is because, the average short parking time at public locations makes level 2 mode unable to supply enough energy. And at work locations, despite users choosing level 2 mode more frequently, DCFC demand remains slightly larger than level 2 demand, since the charging speed of DCFC is 24 times of the level 2 mode. In other words, the need for fast charging seems to dominate over users' dislike for it.



(a) willingness to pay for charging rate. (b) neutral to fast charge. (c) willingness to accept for charging rate.

Figure 7: Charging demand share of three scenarios with different preferences to charging rates.

4.2.3 Effect of work/public charging availability rate

A low charging availability rate can largely reduce the charging demand at work/public locations. Fig. 8 depicts the work/public demand share to be 58% if EVSEs are perfectly accessible (availability rate 100%). This demand share decreases to 25% if EVSEs at work/public locations are rarely accessible (availability rate is 20%). The results imply that there are strong needs to charge at work/public locations, however, these needs can be restricted by the shortage of EVSEs.

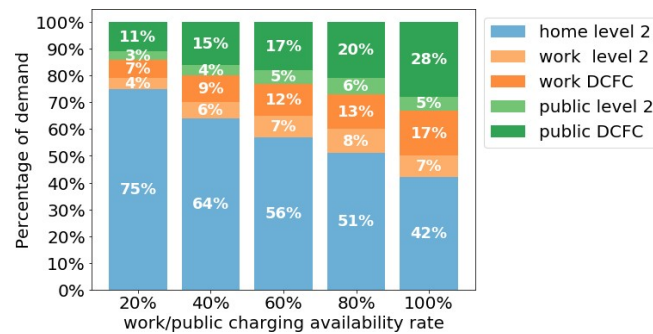


Figure 8: Demand share of each charging mode under different work/public charging availability rates.

4.3 Discussion

The results suggest that work/public charging has substantial potential demands. If the EVSEs are perfectly accessible, the charging demand at work/public locations can reach up to 64.5% of the total demand. This implies users' strong charging needs at work/public, which is calling for the placement of EVSEs at work/public locations.

Optimal placement of EVSEs is important to satisfy the demand at work/public. The results show that the low availability of EVSEs can decrease the work/public demand by 33%. These unsatisfied charging needs could discourage BEV adoption. Thus, optimal EVSE planning—not only installing a sufficient number of EVSEs but also placing them at the 'right' locations—is necessary for efficiently providing highly accessible EVSEs at work/public.

A clear understanding of users charging behavior in the real world can be crucial for optimal EVSE planning. This is because charging demand is highly affected by users charging behavior. For instance, compared to a low-risk sensitive scenario, if users have a high-risk sensitivity, 49% to 91% more level 2 chargers at non-residential areas and 50% more DCFCs at public would be required to satisfy peak-hour demand. Moreover, users with a preference for fast charging rates ask for 45% more DCFCs during peak hours.

DCFCs are expected to provide robust demand at work/public locations. Due to their ability to supply a large amount of energy in a short time, DCFCs take the biggest portion of work/public demand across all scenarios. In the scenario when users prefer fast charging, DCFCs can even supply more than 50% of the total demand. These results imply the predominant role of DCFCs in the future EVSE market.

As for electricity load management, it should be aware of users' extreme charging behavior. For instance, when users are high-risk sensitive, the DCFC peak demand at public is 50% higher than in the low-risk sensitive scenario. And when users have a preference over high charging power, 17.3% more energy is required for DCFCs than when users dislike high charging power. These additional demands could add complexity to electricity load management, especially during peak hours.

5 Conclusion

Accurately estimating the spatio-temporal distribution of the BEV's charging demand is important for optimal EVSE planning and electricity load management. This research proposes an activity-based BEV charging demand simulation model which gives more realistic estimations of high-resolution spatio-temporal demand in real-world applications. A case study in the Atlanta metropolitan area demonstrates the properties of the demand distribution. The results reveal that the charging demand at work/public locations can take more than half of the total charging demand, which implies the necessity of installing

EVSEs at work/public locations. The research also shows that users' charging behavior affects the spatio-temporal demand distribution significantly. Thus, a thorough consideration of users charging behavior is important for optimal EVSE planning and electricity load prediction.

One limitation of this research is the lack of real-world data for calibrating the charging behavior model. Besides, it would be worth studying the effect of different market share of BEV and electricity price setting. These would be expected if real-world data is collected from a mature future BEV market.

Acknowledgments

The contents of this paper reflect the views of the authors, who are responsible for the facts and the accuracy of the information presented herein. This document is disseminated in the interest of information exchange. The work is funded partially by a grant from the U.S. Department of Transportation's University Transportation Centers Program. However, the U.S. Government assumes no liability for the contents or use thereof.

References

- [1] Kelly FJ, Zhu T. Transport solutions for cleaner air. *Science*. 2016;352(6288):934-6.
- [2] Inventory of U.S. Greenhouse Gas Emissions and Sinks: 1990-2019. US Environmental Protection Agency; 2021.
- [3] Dominković DF, Bačeković I, Pedersen AS, Krajačić G. The future of transportation in sustainable energy systems: Opportunities and barriers in a clean energy transition. *Renewable and Sustainable Energy Reviews*. 2018;82:1823-38.
- [4] Tayarani M, Poorfakhraei A, Nadafianshahamabadi R, Rowangould G. Can regional transportation and land-use planning achieve deep reductions in GHG emissions from vehicles? *Transportation Research Part D: Transport and Environment*. 2018;63:222-35.
- [5] Isik M, Dodder R, Kaplan PO. Transportation emissions scenarios for New York City under different carbon intensities of electricity and electric vehicle adoption rates. *Nature Energy*. 2021;6(1):92-104.
- [6] Tessum CW, Hill JD, Marshall JD. Life cycle air quality impacts of conventional and alternative light-duty transportation in the United States. *Proceedings of the National Academy of Sciences*. 2014;111(52):18490-5.
- [7] Richardson DB. Electric vehicles and the electric grid: A review of modeling approaches, Impacts, and renewable energy integration. *Renewable and Sustainable Energy Reviews*. 2013;19:247-54.
- [8] Pan S, Fulton LM, Roy A, Jung J, Choi Y, Gao HO. Shared use of electric autonomous vehicles: Air quality and health impacts of future mobility in the United States. *Renewable and Sustainable Energy Reviews*. 2021;149:111380.
- [9] U S Department of Energy ORNL. Hybrid and Electric Vehicle Sales. *Transportation Energy Data Book, Edition 381*. 2019:table 6.2.
- [10] Das H, Rahman M, Li S, Tan C. Electric vehicles standards, charging infrastructure, and impact on grid integration: A technological review. *Renewable and Sustainable Energy Reviews*. 2020;120:109618.
- [11] Wee S, Coffman M, La Croix S. Do electric vehicle incentives matter? Evidence from the 50 US states. *Research Policy*. 2018;47(9):1601-10.
- [12] Wood EW, Rames CL, Muratori M, Srinivasa Raghavan S, Melaina MW. National plug-in electric vehicle infrastructure analysis. 2017.
- [13] Crabtree G. The coming electric vehicle transformation. *Science*. 2019;366(6464):422-4.
- [14] Shareef H, Islam MM, Mohamed A. A review of the stage-of-the-art charging technologies, placement methodologies, and impacts of electric vehicles. *Renewable and Sustainable Energy Reviews*. 2016;64:403-20.
- [15] IEA. Electricity demand from the electric vehicle fleet by country and region, 2030. 2020.
- [16] Majidpour M, Qiu C, Chu P, Pota HR, Gadh R. Forecasting the EV charging load based on customer profile or station measurement? *Applied Energy*. 2016;163:134-41.
- [17] Quirós-Tortós J, Espinosa AN, Ochoa LF, Butler T. Statistical Representation of EV Charging: Real Data Analysis and Applications. In: *2018 Power Systems Computation Conference (PSCC)*; 2018. p. 1-7.
- [18] Xydas E, Marmaras C, Cipcigan LM, Jenkins N, Carroll S, Barker M. A data-driven approach for characterising the charging demand of electric vehicles: A UK case study. *Applied Energy*. 2016;162:763-71.
- [19] Lin H, Fu K, Wang Y, Sun Q, Li H, Hu Y, et al. Characteristics of electric vehicle charging demand at multiple types of location-Application of an agent-based trip chain model. *Energy*. 2019;188:116122.
- [20] Liang H, Lee Z, Li G. A Calculation Model of Charge and Discharge Capacity of Electric Vehicle Cluster Based on Trip Chain. *IEEE Access*. 2020;8:142026-42.
- [21] Yi T, Zhang C, Lin T, Liu J. Research on the spatial-temporal distribution of electric vehicle charging load demand: A case study in China. *Journal of Cleaner Production*. 2020;242:118457.
- [22] Xiang Y, Jiang Z, Gu C, Teng F, Wei X, Wang Y. Electric vehicle charging in smart grid: A

- spatial-temporal simulation method. *Energy*. 2019;189:116221.
- [23] Wang D, Gao J, Li P, Wang B, Zhang C, Saxena S. Modeling of plug-in electric vehicle travel patterns and charging load based on trip chain generation. *Journal of Power Sources*. 2017;359:468-79.
- [24] Shun T, Kunyu L, Xiangning X, Jianfeng W, Yang Y, Jian Z. Charging demand for electric vehicle based on stochastic analysis of trip chain. *IET Generation, Transmission & Distribution*. 2016;10(11):2689-98.
- [25] Tang D, Wang P. Probabilistic modeling of nodal charging demand based on spatial-temporal dynamics of moving electric vehicles. *IEEE Transactions on Smart Grid*. 2015;7(2):627-36.
- [26] Wang D, Guan X, Wu J, Gao J. Analysis of multi-location PEV charging behaviors based on trip chain generation. In: 2014 IEEE International Conference on Automation Science and Engineering (CASE). IEEE; 2014. p. 151-6.
- [27] Jahangir H, Tayarani H, Ahmadian A, Golkar MA, Miret J, Tayarani M, et al. Charging demand of plug-in electric vehicles: Forecasting travel behavior based on a novel rough artificial neural network approach. *Journal of Cleaner Production*. 2019;229:1029-44.
- [28] Paevere P, Higgins A, Ren Z, Horn M, Grozev G, McNamara C. Spatio-temporal modelling of electric vehicle charging demand and impacts on peak household electrical load. *Sustainability Science*. 2014;9(1):61-76.
- [29] Kelly JC, MacDonald JS, Keoleian GA. Time-dependent plug-in hybrid electric vehicle charging based on national driving patterns and demographics. *Applied Energy*. 2012;94:395-405.
- [30] Yang J, Wu F, Yan J, Lin Y, Zhan X, Chen L, et al. Charging demand analysis framework for electric vehicles considering the bounded rationality behavior of users. *International Journal of Electrical Power & Energy Systems*. 2020;119:105952.
- [31] Xing Q, Chen Z, Zhang Z, Huang X, Leng Z, Sun K, et al. Charging demand forecasting model for electric vehicles based on online ride-hailing trip data. *IEEE Access*. 2019;7:137390-409.
- [32] Amini MH, Kargarian A, Karabasoglu O. ARIMA-based decoupled time series forecasting of electric vehicle charging demand for stochastic power system operation. *Electric Power Systems Research*. 2016;140:378-90.
- [33] Pareschi G, Küng L, Georges G, Boulouchos K. Are travel surveys a good basis for EV models? Validation of simulated charging profiles against empirical data. *Applied Energy*. 2020;275:115318.
- [34] Canizes B, Soares J, Costa A, Pinto T, Lezama F, Novais P, et al. Electric vehicles' user charging behaviour simulator for a smart city. *Energies*. 2019;12(8):1470.
- [35] Hu L, Dong J, Lin Z. Modeling charging behavior of battery electric vehicle drivers: A cumulative prospect theory based approach. *Transportation Research Part C: Emerging Technologies*. 2019;102:474-89.
- [36] Omran NG, Filizadeh S. Location-based forecasting of vehicular charging load on the distribution system. *IEEE Transactions on Smart Grid*. 2013;5(2):632-41.
- [37] Shahidinejad S, Filizadeh S, Bibeau E. Profile of charging load on the grid due to plug-in vehicles. *IEEE Transactions on Smart Grid*. 2011;3(1):135-41.
- [38] Sheppard C, Waraich R, Campbell A, Pozdnukov A, Gopal AR. Modeling plug-in electric vehicle charging demand with BEAM: The framework for behavior energy autonomy mobility. 2017.
- [39] Fazeli SS, Venkatachalam S, Chinnam RB, Murat A. Two-stage stochastic choice modeling approach for electric vehicle charging station network design in urban communities. *IEEE Transactions on Intelligent Transportation Systems*. 2020:1-16.
- [40] Pagany R, Marquardt A, Zink R. Electric Charging Demand Location Model—A User-and Destination-Based Locating Approach for Electric Vehicle Charging Stations. *Sustainability*. 2019;11(8):2301.
- [41] Commission AR, et al. Activity-Based Travel Model Specifications: Coordinated Travel—Regional Activity Based Modeling Platform (CT-RAMP) for the Atlanta Region. Online at:

<http://documents.atlantaregional.com/The-Atlanta-Region-s-Plan/RTP/abmspecification-report.pdf>. 2012.

- [42] Wen Y, MacKenzie D, Keith DR. Modeling the charging choices of battery electric vehicle drivers by using stated preference data. *Transportation Research Record*. 2016;2572(1):47-55.
- [43] McFadden D. Conditional logit analysis of qualitative choice behavior. In: *Frontiers in econometrics*. Academic Press, INC.; 1974. .
- [44] Franke T, Krems JF. Interacting with limited mobility resources: Psychological range levels in electric vehicle use. *Transportation Research Part A: Policy and Practice*. 2013;48:109-22.
- [45] Franke T, Neumann I, Bühler F, Cocron P, Krems JF. Experiencing range in an electric vehicle: Understanding psychological barriers. *Applied Psychology*. 2012;61(3):368-91.
- [46] Jabeen F, Olaru D, Smith B, Braunl T, Speidel S. Electric vehicle battery charging behaviour: Findings from a driver survey. In: *Proceedings of the Australasian Transport Research Forum*; 2013. .
- [47] Abdel-Monem M, Trad K, Omar N, Hegazy O, Van den Bossche P, Van Mierlo J. Influence analysis of static and dynamic fast-charging current profiles on ageing performance of commercial lithium-ion batteries. *Energy*. 2017;120:179-91.
- [48] Daina N, Sivakumar A, Polak JW. Electric vehicle charging choices: Modelling and implications for smart charging services. *Transportation Research Part C: Emerging Technologies*. 2017;81:36-56.
- [49] Chakraborty D, Bunch DS, Lee JH, Tal G. Demand drivers for charging infrastructure-charging behavior of plug-in electric vehicle commuters. *Transportation Research Part D: Transport and Environment*. 2019;76:255-72.
- [50] Sun XH, Yamamoto T, Morikawa T. Charge timing choice behavior of battery electric vehicle users. *Transportation Research Part D: Transport and Environment*. 2015;37:97-107.
- [51] Franke T, Krems JF. Understanding charging behaviour of electric vehicle users. *Transportation Research Part F: Traffic Psychology and Behaviour*. 2013;21:75-89.
- [52] Yan Q, Manickam I, Kezunovic M, Xie L. A multi-tiered real-time pricing algorithm for electric vehicle charging stations. In: *2014 IEEE Transportation Electrification Conference and Expo (ITEC)*. IEEE; 2014. p. 1-6.